

## Calculation of surface stress for fcc transition metals

J. Kollár and L. Vitos

Research Institute for Solid State Physics and Optics, P.O. Box 49, H-1525 Budapest, Hungary

J. M. Osorio-Guillén and R. Ahuja

Condensed Matter Theory Group, Department of Physics, Uppsala University, Box 530, S-751 21 Uppsala, Sweden

(Received 29 July 2003; published 18 December 2003)

Using the density functional theory, formulated within the framework of the exact muffin-tin orbitals method, we have calculated the surface stress for the (111) free surfaces of the fcc  $4d$  and  $5d$  transition metals. Good agreement is obtained with the available *ab initio* data for Pd, Ir, and Au, while for Pt we predict a surface stress, which is about 33% lower compared to former theoretical results. The present surface stress values for the  $4d$  and  $5d$  fcc metals show the typical trend characteristic for the cohesive or surface energies of  $d$  series.

DOI: 10.1103/PhysRevB.68.245417

PACS number(s): 68.35.Gy, 71.15.Nc, 73.20.-r

### I. INTRODUCTION

The surface stress and the surface energy play basic roles in understanding and modeling phenomena taking place on solid surfaces. One of the most important driving forces of surface reconstruction, for instance, is the surface stress. Nonzero surface stress arises when the two-dimensional surface layer energetically favors a different lattice constant compared to that in the bulk. By definition, the surface stress is negative or compressive when the surface layer tends to expand, and positive or tensile when a smaller lattice constant is preferred.

Although different techniques have been developed to measure the changes of the surface stress when the surface is exposed to adsorbates, or when it undergoes reconstruction,<sup>1,2</sup> it is not yet possible to determine the absolute value of the surface stress experimentally with acceptable accuracy.<sup>3-8</sup> The same applies for the surface free energy, and therefore it is of increasing importance that substantial progress be achieved in first principles calculations for the surface energy<sup>9</sup> and the surface stress.<sup>10-13</sup>

The aim of this work is to present a uniform and efficient method to calculate surface stress and to apply it to the determination of the surface stress on (111) surface facets for fcc  $4d$  and  $5d$  transition metals. In the first part of the paper we briefly review the theory of the surface stress tensor, the employed *ab initio* total energy method, and the most relevant numerical details of our calculations. In the second part we present and discuss our results, and compare them to former *ab initio* and available experimental data. In the case of Pt we obtain significantly smaller surface stress values compared to some of the earlier calculations. We find that in our calculation the surface stress exhibits similar trends for Rh, Pd, Ag and for Ir, Pt, Au as the surface energy or the bulk cohesive energy for the late transition metals.

### II. SURFACE STRESS

The change of the total energy of a system during the  $\delta\epsilon_{ij}$  change of the deformation tensor is given by

$$\delta E = \int \sum_{ij} \sigma_{ij}(\mathbf{r}) \delta \epsilon_{ij} d\mathbf{r}, \quad (1)$$

where  $\sigma_{ij}(\mathbf{r})$  stands for the stress tensor at point  $\mathbf{r} = (x, y, z)$ . Using a slab geometry and assuming periodicity in directions  $x$  and  $y$  we have

$$\delta E = A \int_{-d/2}^{d/2} \sum_{ij} \tau_{ij}(z) \delta \epsilon_{ij} dz. \quad (2)$$

Here  $z$  is perpendicular to the surface of the slab,  $d$  stands for the thickness of the slab,  $A$  is the surface area, and the  $\tau_{ij}(z)$  are the components of the “slab” stress tensor introduced as

$$\tau_{ij}(z) = \frac{1}{A} \int \sigma_{ij}(\mathbf{r}) dx dy. \quad (3)$$

The surface stress tensor is defined<sup>2</sup> from  $\tau_{ij}(z)$  by

$$\tau_{ij}^{(s)} = \int [\tau_{ij}(z) - \tau_{ij}^{(b)}] dz, \quad (4)$$

where  $\tau_{ij}^{(b)}$  denotes the value of the “slab” stress tensor in the bulk region, i.e., far from the surface. In terms of the surface stress tensor  $\tau_{ij}^{(s)}$ , Eq. (2) can be separated into two parts, viz.

$$\delta E = 2 \delta E^{(s)} + \delta E^{(b)} = 2A \sum_{ij} \tau_{ij}^{(s)} \delta \epsilon_{ij} + Ad \sum_{ij} \tau_{ij}^{(b)} \delta \epsilon_{ij}. \quad (5)$$

The factor 2 arises from the two surface facets of the slab. Thus knowing the change of the bulk and the slab energy, we can derive  $\delta E^{(s)}$  related to the  $\delta \epsilon_{ij}$  change of the deformation tensor, i.e.,

$$\delta E^{(s)} = \frac{1}{2} [\delta E - \delta E^{(b)}] = A \sum_{ij} \tau_{ij}^{(s)} \delta \epsilon_{ij} \quad (6)$$

and

$$\tau_{ij}^{(s)} = \frac{1}{A} \frac{\partial E^{(s)}}{\partial \epsilon_{ij}}. \quad (7)$$

Using the relation  $E^{(s)} = A\gamma$ , where  $\gamma$  is the surface energy defined as the reversible work per unit area to create a surface, we can write

$$\tau_{ij}^{(s)} = \frac{1}{A} \frac{\partial A \gamma}{\partial \epsilon_{ij}} = \gamma \delta_{ij} + \frac{\partial \gamma}{\partial \epsilon_{ij}}, \quad (8)$$

where  $\partial \gamma / \partial \epsilon_{ij}$  is the residual surface stress. This is the Shuttleworth equation, expressing that the surface stress is the reversible work per area to stretch the surface elastically.

It is apparent from the definitions that the surface stress and surface energy are of different natures. In the case of stable solids the free energy of a surface is always positive, otherwise the solid would gain energy by fragmentation. The surface stress, on the other hand, can either be positive or negative. We note that for a liquid, the surface free energy and the surface stress are equal due to the fact that in this case the surface energy does not change when the surface is strained, i.e.,  $\partial \gamma / \partial \epsilon_{ij} = 0$ . These two quantities are frequently referred to by the common name ‘‘surface tension.’’

### III. METHOD OF TOTAL ENERGY CALCULATION

Our calculations are based on the density functional theory.<sup>14</sup> The Kohn-Sham equations<sup>15</sup> are solved using the recently developed exact muffin-tin orbitals (EMTO) method. The original formulation of the exact muffin-tin orbitals theory can be found in Refs. 16,17, while the self-consistent implementation of the theory, within the spherical cell approximation, is given in Refs. 18,19. Therefore here we outline only the most important details of the method.

The EMTO theory is an improved screened Korringa-Kohn-Rostoker (KKR) method, where the one-electron potential is represented by optimized overlapping muffin-tin (OOMT) potential. This potential ensures a more accurate description of the full potential compared to the conventional spherically symmetric potentials. For the OOMT potential, the one-electron states and thus the one-electron kinetic energies are calculated exactly within the frame of the density functional theory. As an output of the EMTO calculation, we determine the self-consistent Green’s function of the system and the complete, nonspherically symmetric charge density. This density is normalized within space filling, nonoverlapping cells centered around each lattice site, and it is continuous and continuously differentiable in all space.<sup>18</sup> In the EMTO method the total kinetic energy is given by the Kohn-Sham kinetic energy obtained from the one-electron equations. The Coulomb part of the total energy and the exchange-correlation energy functional are evaluated from the total density using the full charge density and shape functional techniques, as described in, e.g., Refs. 18,20.

### IV. NUMERICAL DETAILS

The surface stress tensor of the fcc (111) surface is calculated using Eq. (6). We carry out supercell calculations with slab geometry, and during the ‘‘stretching’’ deformation we elongate the lattice vectors lying in the surface plane by  $\epsilon$ , while the third lattice vector, which determines the layer-

layer distance, is kept fixed. For this distortion the deformation tensor has the form

$$\epsilon_{ij} = \begin{bmatrix} \epsilon & 0 & 0 \\ 0 & \epsilon & 0 \\ 0 & 0 & 0 \end{bmatrix}. \quad (9)$$

In this case the energy changes  $\delta E$  and  $\delta E^{(b)}$  are given as a function of  $\epsilon$ . First we calculate the total energies of slab and bulk systems for several different  $\epsilon$  values, and next, in order to minimize the numerical noises, fit a polynomial to the calculated mesh points, i.e., we make the approximation

$$\delta E \approx c_0 + c_1 \epsilon + c_2 \epsilon^2 + \dots \quad (10)$$

Thus, the surface stress  $\tau^{(s)}$  is determined by the linear coefficients of the slab and bulk energies, viz.

$$\tau^{(s)} = \frac{c_1 - c_1^{(b)}}{2A}. \quad (11)$$

In the present surface stress calculation the EMTO simulations have been performed for unreconstructed, ideal fcc (111) surfaces. The surfaces have been modeled by a supercell geometry with 12 layers consisting of 8 atomic and 4 vacuum layers, describing the vacuum region. In order to test the layer convergence of the total energies, in some cases we have increased the number of layers up to 18. The volumes of the undistorted supercells have been fixed by separate bulk calculations, and the linear coefficients from Eq. (10) have been determined using five deformations  $\epsilon = 0.0, \pm 0.01, \text{ and } \pm 0.02$ . The area of the two-dimensional unit cell on (111) surface is  $A = (\sqrt{3}/4)a_{\text{th}}^2$ , where  $a_{\text{th}}$  denotes the theoretical equilibrium lattice constant.

In the self-consistent EMTO total energy calculations the one-electron equations have been solved within the scalar-relativistic and soft-core approximations. The Green’s function has been calculated for 32 complex energy points distributed exponentially on a semicircle. We have used 573  $k$  points in the irreducible part of the two-dimensional hexagonal Brillouin-zone. The total charge density has been expanded in spherical harmonics, including terms up to  $l_{\text{max}} = 10$ , and the shape function components have been truncated at  $l_{\text{max}}^s = 30$ . For the exchange-correlation term we have used the local density approximation (LDA),<sup>21</sup> which has proved accurate for nonmagnetic late transition metals.<sup>22</sup>

The calculation of the surface stress is illustrated in Fig. 1 for Pt at the equilibrium volume ( $w_{\text{eq}}$ ) and at a slightly smaller volume, to show the effect of volume change on the energy curves. We can see from the figure that at the equilibrium volume the bulk total energy curve has a minimum at  $\epsilon = 0$  (i.e.,  $c_1^{(b)} = 0$ ), while the slab energy has a minimum at  $\epsilon < 0$  (i.e.,  $c_1 > 0$ ), exhibiting a tensile surface stress. Note, that for  $w < w_{\text{eq}}$  the bulk and slab minima are shifted, but the difference between the slopes of the energy curves is not significantly altered.

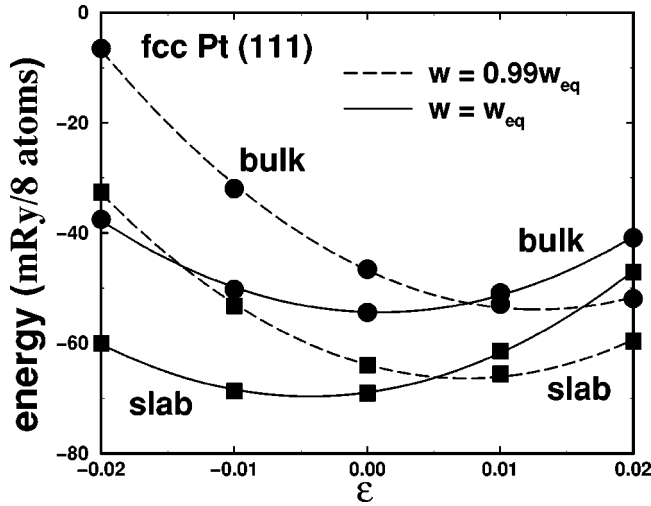


FIG. 1. Total slab and bulk energies for Pt as a function of the deformation parameter defined in Eq. (9) for the fcc(111) surface, at the equilibrium radius  $w_{eq}$  and  $0.99w_{eq}$ .

## V. RESULTS AND DISCUSSION

The present surface stress results for the (111) surfaces of the fcc  $4d$  and  $5d$  transition metals, together with the former *ab initio* theoretical data, are listed in Table I and plotted in Figs. 2 and 3. For completeness, we also included in table the available experimental surface stress data and the calculated surface energies.

The experimental surface stress values have been determined from the observed contraction of the metal particles with diameters 1.4–5 nm (Ref. 3) for Pd, 3–17.8 nm (Ref. 4) and  $\sim 3$  nm (Ref. 5) for Ag, 1.9–12.2 nm (Ref. 6) and 3–40 nm (Ref. 7) for Pt, and 3.5–12.5 nm (Ref. 8) and 3–40 nm (Ref. 7) for Au. Except for Pd, where the measured value is high by about a factor of 2 compared with the *ab initio* results, the experimental values show a significant scattering around the theoretical data. The discrepancy between differ-

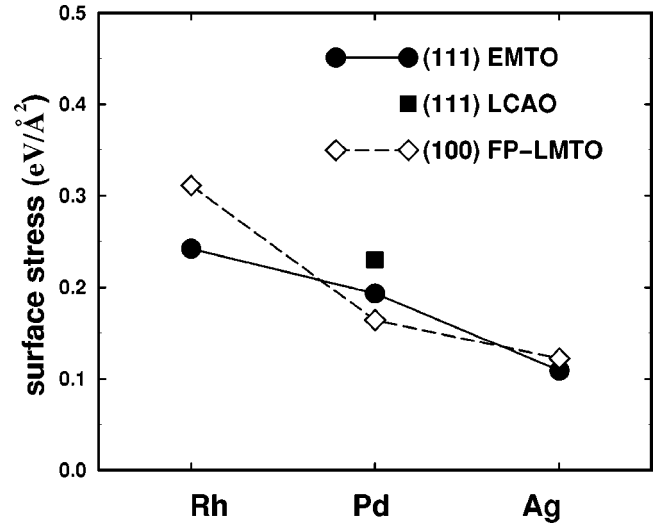


FIG. 2. Surface stress for the fcc(111) surface of  $4d$  transition metals. The present EMTO result for Pd is compared to LCAO value from Ref. 13. The FP-LMTO results (Ref. 11) for the (100) facets are included for reference.

ent experimental values can be attributed to poor vacuum conditions,<sup>2</sup> but also to the surface and bulk reconstruction driven by size effects.<sup>23,24</sup> Note, however, the good agreement between the present theoretical results and the data for Pt and Au obtained in experiments involving particles with relatively large mean sizes.<sup>7</sup>

For Pd the 16% relative difference between the present value and Feibelman's result,<sup>13</sup> obtained using the linear combination of atomic orbitals (LCAO) method, is satisfactory. In the case of Ir and Au the agreement with former theoretical values is also very good. The relative differences between our and the pseudopotential results by Needs and Mansfield<sup>10</sup> are 6 and 8%, respectively. However, for Pt we have found a large discrepancy between the present EMTO value and the pseudopotential<sup>10,25</sup> and LCAO (Ref. 13) results.

TABLE I. Surface energy and surface stress values for the (111) surface facets of fcc  $4d$  and  $5d$  transition metals calculated by the exact muffin-tin orbitals method. For comparison we have included the available full potential and experimental results.

Metal	EMTO		Full-potential		Experimental
	$\gamma$ (meV/Å <sup>2</sup> )	$\tau$ (meV/Å <sup>2</sup> )	$\gamma$ (meV/Å <sup>2</sup> )	$\tau$ (meV/Å <sup>2</sup> )	
Rh	200	242	158 <sup>a</sup>		
Pd	141	193	102 <sup>a</sup>	230 <sup>b</sup>	375 ± 56 <sup>e</sup>
Ag	85	109	76 <sup>a</sup>		88 <sup>f</sup> , 399 <sup>g</sup>
Ir	256	312	204 <sup>c</sup>	331 <sup>c</sup>	
Pt	188	234	137 <sup>c</sup>	392 <sup>b</sup> , 350 <sup>c</sup> , 370 <sup>d</sup>	161 <sup>h</sup> , 240 ± 44 <sup>i</sup> , 275 ± 62 <sup>i</sup>
Au	105	160	78 <sup>c</sup>	173 <sup>c</sup>	73 <sup>j</sup> , 192 ± 44 <sup>i</sup> , 199 ± 62 <sup>i</sup>

<sup>a</sup>LMTO, Methfessel *et al.* (Ref. 28).

<sup>b</sup>LCAO, Feibelman (Ref. 13).

<sup>c</sup>Pseudopotential, Needs and Mansfield (Ref. 10).

<sup>d</sup>Pseudopotential, Boisvert *et al.* (Ref. 25).

<sup>e</sup>Lamber *et al.* (Ref. 3).

<sup>f</sup>Wassermann *et al.* (Ref. 4).

<sup>g</sup>Berry (Ref. 5).

<sup>h</sup>Wassermann *et al.* (Ref. 6).

<sup>i</sup>Solliard *et al.* (Ref. 7).

<sup>j</sup>Mays *et al.* (Ref. 8).

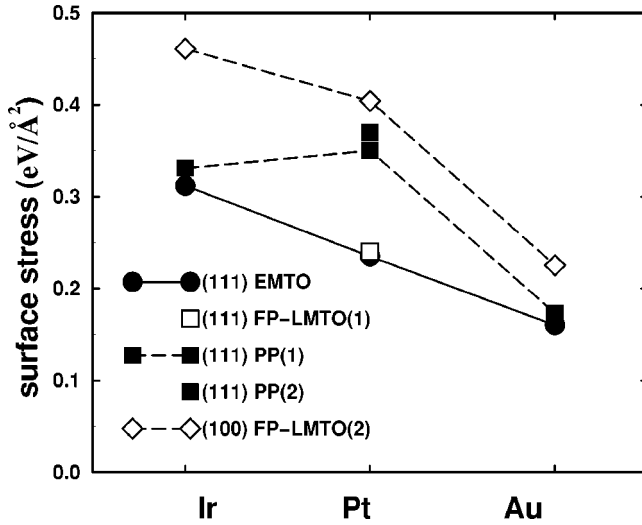


FIG. 3. Surface stress for the fcc(111) surface facets of 5d transition metals. The present EMTO and full-potential results [FP-LMTO(1)] are compared to earlier *ab initio* data: PP(1) and PP(2) are the pseudopotential results from Refs. 10 and 25, respectively. The full-potential results (Ref. 11) [FP-LMTO(2)] for the (100) facets are included for reference.

In order to test the accuracy of the present surface stress values, in addition to the above EMTO calculation, we have also carried out an independent full potential linear muffin-tin orbitals (FP-LMTO) calculation for Pt. Details about the employed FP-LMTO method can be found in Refs. 26,27. In the FP-LMTO calculation we have used exactly the same supercell and total energy functional as in the case of the EMTO. The obtained surface stress for Pt is 240 meV/Å<sup>2</sup>, which is in complete agreement with our EMTO result of 234 meV/Å<sup>2</sup>.

In both EMTO and FP-LMTO calculations the relaxations of the surface layers were neglected. Using the EMTO method we investigated the top layer relaxation of the (111) surfaces of late 4d transition metals. The calculated changes in the interlayer distances are of order of 1%, in good agreement with former theoretical findings.<sup>28</sup> The effect of surface relaxation on the surface energies is found to be around 5%. Therefore, we estimate that the errors in the present *ab initio* surface stress values due to the neglect of the relaxations should be below 10%.

To understand the nature and the physical background of surface stress in transition metals, we return to the simple picture of cohesion<sup>29</sup> in bulk transition metals. According to this model the equilibrium value of the bond length arises from the balance of the repulsive pressure of the nearly free electronlike *s,p* electrons, and the attractive pressure contribution of the more localized *d* electrons. The latter contribution exhibits the well-known parabolic trend throughout the transition series. This simple qualitative picture was verified by *ab initio* calculations,<sup>30</sup> where the partial pressure contributions had been expressed in terms of the band structure parameters using the pressure formula. If we look at the surface layer of our fcc (111) transition metal slabs, we can generally say that the total number of electrons is reduced relative to the bulk, but the number of *d* electrons remains

TABLE II. The change in the total number of electrons  $\Delta n$  and in the number of *d* electrons  $\Delta n_d$  for the top layer of the (111) surfaces of fcc 4d and 5d transition metals relative to the bulk values.

Metal	$\Delta n$	$\Delta n_d$
Rh	-0.15	0.06
Pd	-0.12	0.08
Ag	-0.12	0.03
Ir	-0.15	0.05
Pt	-0.11	0.06
Au	-0.10	0.02

approximately unchanged (slightly increases). The obtained changes in the total number of electrons and in the number of *d* electrons for fcc 4d and 5d metals are shown in Table II. In the spirit of the above model for cohesion, this means that in the surface layer the repulsive pressure contribution of the *s,p* electrons is reduced and the unchanged attractive *d*-band contribution results in a tensile surface stress. We mention that this picture is different from that by Fiorentini *et al.*,<sup>11</sup> who have found that the number of *d* electrons, and thus, for late transition metals, the number of nonbonding *d* orbitals is reduced in the surface layer, resulting in a tensile surface stress.

The above simple bond picture explains the present trend obtained for the surface stress, see Figs. 2 and 3. Moreover, we find that the theoretical surface stress values for different surface facets show similar behavior in terms of the number of *d* electrons. This is illustrated in Figs. 2 and 3, where we compared the EMTO surface stress results for the (111) facets to the FP-LMTO results for the (100) surface facets.<sup>11</sup>

## VI. CONCLUSIONS

Using the EMTO total energy method we have calculated the surface stress on the (111) surface of fcc 4d and 5d transition metals. For Pt an additional full potential calculations confirms the high accuracy of the present theoretical results. We find that the general agreement between the EMTO results and the former theoretical data is reasonable. The obtained trend of the surface stress follows the characteristic behavior of the surface energy of the transition metals, in good accordance the simple picture of the cohesion in transition metals.

## ACKNOWLEDGMENTS

This work was supported by the research Project No. OTKA T035043 of the Hungarian Scientific Research Fund, the Hungarian Academy of Science and the EC Center of Excellence program (Grant No. ICA1-CT-2000-70029). The Swedish Research Council, the Swedish Foundation for Strategic Research and The Royal Swedish Academy of Sciences are also acknowledged for financial support. The computer simulations were done at the Hungarian and Swedish National Supercomputer Centers.

- <sup>1</sup>C.E. Bach, M. Giesen, H. Ibach, and T.L. Einstein, *Phys. Rev. Lett.* **78**, 4225 (1997).
- <sup>2</sup>H. Ibach, *Surf. Sci. Rep.* **29**, 193 (1997).
- <sup>3</sup>R. Lamber, S. Wetjen, and N.I. Jaeger, *Phys. Rev. B* **51**, 10 968 (1995).
- <sup>4</sup>H.J. Wassermann and J.S. Vermaak, *Surf. Sci.* **22**, 164 (1970).
- <sup>5</sup>C.R. Berry, *Phys. Rev.* **88**, 596 (1952).
- <sup>6</sup>H.J. Wassermann and J.S. Vermaak, *Surf. Sci.* **32**, 168 (1972).
- <sup>7</sup>C. Solliard and M. Flueli, *Surf. Sci.* **156**, 487 (1985).
- <sup>8</sup>C.W. Mays, J.S. Vermaak, and D. Kuhlmann-Wilsdorf, *Surf. Sci.* **12**, 134 (1968); J.S. Vermaak, C.W. Mays, and D. Kuhlmann-Wilsdorf, *ibid.* **12**, 128 (1968).
- <sup>9</sup>See, e.g., L. Vitos, A.V. Ruban, H.L. Skriver, and J. Kollár, *Surf. Sci.* **411**, 186 (1998), and references therein.
- <sup>10</sup>R.J. Needs and M. Mansfield, *J. Phys.: Condens. Matter* **1**, 7555 (1989).
- <sup>11</sup>V. Fiorentini, M. Methfessel, and M. Scheffler, *Phys. Rev. Lett.* **71**, 1051 (1993).
- <sup>12</sup>P.J. Feibelman, *Phys. Rev. B* **50**, 1908 (1994).
- <sup>13</sup>P.J. Feibelman, *Phys. Rev. B* **51**, 17 867 (1995).
- <sup>14</sup>P. Hohenberg and W. Kohn, *Phys. Rev.* **136B**, 864 (1964).
- <sup>15</sup>W. Kohn and L.J. Sham, *Phys. Rev.* **140A**, 1133 (1965).
- <sup>16</sup>O.K. Andersen, O. Jepsen, and G. Krier, in *Methods of Electronic Structure Calculations*, edited by V. Kumar, O.K. Andersen, and A. Mookerjee (World Scientific, Singapore, 1994), p. 63.
- <sup>17</sup>O.K. Andersen, C. Arcangeli, R.W. Tank, T. Saha-Dasgupta, G. Krier, O. Jepsen, and I. Dasgupta, in *Tight-binding Approach to Computational Materials Science*, edited by P. E. A. Turchi, A. Gonis, and L. Colombo, *Mater. Res. Soc. Symp. Proc. No. 491* (Materials Research Society, Warrendale, 1998), pp. 3–34.
- <sup>18</sup>L. Vitos, H.L. Skriver, B. Johansson, and J. Kollár, *Comput. Mater. Sci.* **18**, 24 (2000).
- <sup>19</sup>L. Vitos, *Phys. Rev. B* **64**, 014107 (2001).
- <sup>20</sup>J. Kollár, L. Vitos, and H.L. Skriver, in *Electronic Structure and Physical Properties of Solids: The Uses of the LMTO Method*, edited by Hugues Dreyssé, *Lecture Notes in Physics* (Springer, Berlin, 2000), pp. 85–113.
- <sup>21</sup>J.P. Perdew and Y. Wang, *Phys. Rev. B* **45**, 13 244 (1992).
- <sup>22</sup>L. Vitos, B. Johansson, J. Kollár, and H.L. Skriver, *Phys. Rev. B* **62**, 10 046 (2000).
- <sup>23</sup>A. Renou and M. Gillet, *Surf. Sci.* **106**, 27 (1981).
- <sup>24</sup>L. Vitos, B. Johansson, and J. Kollár, *Phys. Rev. B* **62**, R11 957 (2000).
- <sup>25</sup>G. Boisvert, L.J. Lewis, and M. Scheffler, *Phys. Rev. B* **57**, 1881 (1998).
- <sup>26</sup>R. Ahuja, O. Eriksson, J.M. Wills, and B. Johansson, *Phys. Rev. Lett.* **75**, 3473 (1995); J.M. Wills, O. Eriksson, and M. Alouani, in *Electronic Structure and Physical Properties of Solids: The Uses of the LMTO Method*, edited by Hugues Dreyssé, *Lecture Notes in Physics* (Springer, Berlin, 2000), p. 148.
- <sup>27</sup>In the full potential linear muffin-tin orbitals calculations, the electron density and potential were computed without any geometrical approximation. These quantities were expanded in combinations of spherical harmonic functions with a cutoff  $\ell_{\max} = 6$  inside the nonoverlapping muffin-tin spheres and in Fourier series outside the spheres. The muffin-tin sphere occupied approximately 50% of the unit cell. We used separate basis functions for the  $5p$  semicore and  $6s$ ,  $6p$ , and  $5d$  valence states, with corresponding two sets of energy parameters, and the resulting basis formed a single, fully hybridizing basis set. For sampling the irreducible wedge of the Brillouin zone we used the special  $k$ -point method and in order to speed up the convergence we associated each calculated eigenvalue with a Gaussian broadening of 20 mRy width.
- <sup>28</sup>M. Methfessel, D. Hennig, and M. Scheffler, *Phys. Rev. B* **46**, 4816 (1992).
- <sup>29</sup>J. Kollár and G. Solt, *J. Phys. Chem. Solids* **33**, 651 (1972).
- <sup>30</sup>O.K. Andersen, O. Jepsen, and D. Glötzel, in *Highlights of Condensed Matter Theory*, edited by F. Bassani, F. Fumi, and M.P. Tosi (North-Holland, New York, 1985), p. 59.